EUROPEAN ORGANIZATION FOR NUCLEAR RESEARCH
CERN - AB DIVISION

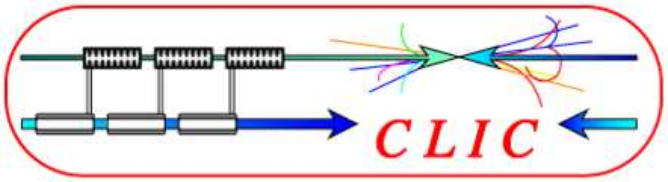

CLIC Note 659

NON-LINEAR OPTIMIZATION OF BEAM LINES

R. Tomás,

CERN-OPEN-2006-023
15/05/2006

Abstract

The current final focus systems of linear colliders have been designed based on the local compensation scheme proposed by P. Raimondi and A. Seryi [1]. However, there exist remaining aberrations that deteriorate the performance of the system. This paper develops a general algorithm for the optimization of beam lines based on the computation of the high orders of the transfer map using MAD-X [2] and PTC [3]. The algorithm is applied to the CLIC [4] Beam Delivery System (BDS).

Geneva, Switzerland
May 15, 2006

1 Introduction

The minimization of aberrations in beam lines has always been a concern. Already in 1973 [5] an analytical approach was derived up to the second order but particle tracking had to be used for higher orders. More recently with the advent of the local compensation scheme [1] the demand for design and optimization algorithms that take into account higher orders has largely increased [6, 7, 8, 9]. This paper describes a general optimization algorithm that takes as figure of merit the rms beam sizes at the end of the beam line. These are analytically computed from the coefficients of the transfer map to an arbitrary order. A particular application to the CLIC BDS is shown as a proof of principle.

2 Mathematical ground

The transfer map between two locations of a beam line is expressed in the form

$$\vec{x}_f = \sum_{jklmn} \vec{X}_{jklmn}\, x_0^j\, p_{x0}^k\, y_0^l\, p_{y0}^m\, \delta_0^n \tag{1}$$

where $\vec{x}_f$ represents the final coordinates (x_f, p_{xf}, y_f, p_{yf}), the initial coordinates are represented with the zero subindex and $\vec{X}_{jklm}$ are the map coefficients of the corresponding final coordinate. The MAD-X version including PTC can provide $\vec{X}_{jklm}$ up to the desired order.
The quadratic standard deviation of the final density distribution, $< x_f^2 >$, is given by the following integral,

$$< x_f^2 >= \int x_f^2 \rho_f dv_f \tag{2}$$

where dv_f represents the differential volume of the final phase space. Assuming that the transfer map is symplectic $\rho_f dv_f = \rho_0 dv_0$ and using eq. (1),

$$< x_f^2 >= \sum_{\substack{jklmn \\ j'k'l'm'n'}} X_{jklmn} X_{j'k'l'm'n'} \int x_0^{j+j'} p_{x0}^{k+k'} y_0^{l+l'} p_{y0}^{m+m'} \delta_0^{n+n'} \rho_0 dv_0 \tag{3}$$

To perform this integral a Gaussian bunch is assumed in the transverse planes (with no orbit offset) and a rectangular distribution is considered in relative energy deviation (for the application to CLIC), given by the following expression,

$$\rho_0 = \frac{e^{-x^2/2\sigma_x^2} e^{-p_x^2/2\sigma_{px}^2} e^{-y^2/2\sigma_y^2} e^{-p_y^2/2\sigma_{py}^2} \Pi\left(\frac{\delta}{\Delta_\delta}\right)}{(2\pi)^2 \sigma_x \sigma_{p_x} \sigma_y \sigma_{p_y} \Delta_\delta} \tag{4}$$

where $\Pi(z)$ is the rectangular function which vanishes when $|z| > 0.5$ and takes the unit value elsewhere. This distribution is representative for the beam expected at the end of the CLIC linac. Note that assuming this particle density imposes constraints in the Twiss functions at the initial location. The horizontal and vertical alpha functions and the closed orbit must be zero. This assumption is fundamental to gain speed in the numerical computation of $< x_f^2 >$ as it will be shown below. Moreover this constraint is not critical since even in the case that the initial location has a non zero α function it is possible to add a matching section meeting our constraints in the new initial point but leaving the initial beam line unchanged.
To compute the integral above the following results are used,

$$\frac{1}{\sqrt{2\pi}\sigma} \int z^n e^{-z^2/2\sigma^2} dz = \begin{cases} \Gamma\left(\frac{1+n}{2}\right) \sigma^n \sqrt{\frac{2^n}{\pi}} & \text{if n even} \\ 0 & \text{if n odd} \end{cases} \tag{5}$$

$$\frac{1}{\sigma}\int z^n \Pi\left(\frac{z}{\sigma}\right) dz = \begin{cases} \frac{1}{n+1}\left(\frac{\sigma}{2}\right)^n & \text{if n even} \\ 0 & \text{if n odd} \end{cases} \tag{6}$$

where $\Gamma(z)$ is the Gamma function. From these equations the gain in computational speed thanks to the chosen symmetry is patent. Using the above equations the standard quadratic deviation of the particle distribution at the end of the beam line is given by

$$\begin{aligned} < x_f^2 > \;=\; & \sum_{jklmn} X_{jklmn}^2 \Gamma\left(\frac{1+2j}{2}\right)\Gamma\left(\frac{1+2k}{2}\right)\Gamma\left(\frac{1+2l}{2}\right)\Gamma\left(\frac{1+2m}{2}\right) \\ & \times \frac{2^{j+k+l+m-2n}}{(2n+1)\pi^2}\sigma_x^{2j}\sigma_{p_x}^{2k}\sigma_y^{2l}\sigma_{p_y}^{2m}\Delta_\delta^{2n} \\ & + \sum_{jklmn>j'k'l'm'n'} 2X_{jklmn}X_{j'k'l'm'n'} \\ & \times \Gamma\left(\frac{1+j+j'}{2}\right)\Gamma\left(\frac{1+k+k'}{2}\right)\Gamma\left(\frac{1+l+l'}{2}\right)\Gamma\left(\frac{1+m+m'}{2}\right) \\ & \times \frac{2^{\frac{j+k+l+m+j'+k'+l'+m'}{2}-n-n'}}{(n+n'+1)\pi^2}\sigma_x^{j+j'}\sigma_{p_x}^{k+k'}\sigma_y^{l+l'}\sigma_{p_y}^{m+m'}\Delta_\delta^{n+n'} \end{aligned} \tag{7}$$

The following sections describe means to extract the information concerning the nature of the aberrations.

2.1 The order-by-order approach

By truncating the map at order q we only consider the coefficients X_{jklmn} such that $j+k+l+m+n \leq q$. The resulting standard deviation is represented by $< x_f^2 >_q$. Thus defined, $\sqrt{< x_f^2 >_1}$ corresponds to rms size given by the linear Twiss functions, $\sqrt{< x_f^2 >_2}$ takes into account the effect of chromatic aberrations and sextupoles, $\sqrt{< x_f^2 >_3}$ incorporates octupolar fields, etc. The final finite size of the bunch is given by $< x_f^2 >_q$ when q tends to infinite. However there must be a finite order p that gives a satisfactory approximation. The evaluation of $< x_f^2 >_q - < x_f^2 >_{q-1}$ gives the contribution of the order q to the final rms beam size. From this contribution the order of the most relevant aberrations is inferred and subsequently the appropriate multipolar correctors are chosen. However the optimum location of the correctors still needs to be identified.

2.2 Chromatic versus achromatic correctors

This section gives the recipe to decide if the correctors should be placed in locations with or without dispersion. $< x_f^2 >_{q,\Delta_\delta=0}$ is defined as the rms size of an monochromatic beam, it is given by

$$< x_f^2 >_{q,\Delta_\delta=0} = \sum_{\substack{jklm \\ j'k'l'm'}} X_{jklm0}X_{j'k'l'm'0}\int x_0^{j+j'} p_{x0}^{k+k'} y_0^{l+l'} p_{y0}^{m+m'} \rho_0 dv_0 \tag{8}$$

with $j+k+l+m \leq q$ and $j'+k'+l'+m' \leq q$. If the contribution from the most relevant order q, $< x_f^2 >_q - < x_f^2 >_{q-1}$, is much larger than its corresponding achromatic contribution, $< x_f^2 >_{q,\Delta_\delta=0} - < x_f^2 >_{q-1,\Delta_\delta=0}$, the correctors should be placed in dispersive locations possibly together with achromatic correctors to cancel the arising geometric aberrations. In the opposite case only achromatic correctors should be placed.

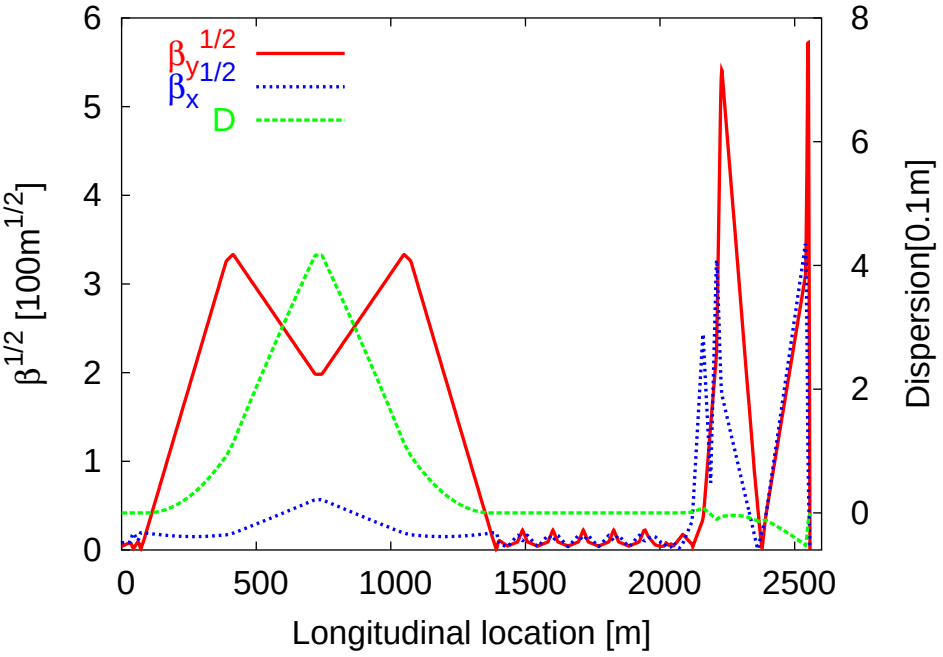

Figure 1: Twiss functions of the CLIC Beam Delivery System.

3 Optimization of the CLIC Beam Delivery System

The CLIC BDS consists of a collimation section and a Final Focus System (FFS). The Twiss functions of the BDS are plotted in Fig 1. The collimation section has a length of about 2 km. The first 70 m serve as a matching section between the main linac and the BDS. After these 70 m the α functions are zero and therefore this location is taken as the initial location for the computation of the transfer map. The horizontal and vertical normalized beam emittances are $\epsilon_x = 68 \times 10^{-8}$ m and $\epsilon_y = 1 \times 10^{-8}$ m, with a relativistic gamma of $\gamma = 3 \times 10^6$. The full energy width of the beam is $\Delta_\delta = 0.01$. The rms beam sizes at the IP are computed using eq. (7) and plotted up to the 9^{th} order in Fig. 2. The nominal beam as well as the achromatic beam ($\Delta_\delta = 0$) are shown leading to the conclusion that most of the aberrations are chromatic. Only sextupolar and octupolar geometric aberrations appear in the vertical plane. It is striking that the vertical aberrations are relevant up to the highest orders. The most relevant horizontal aberrations are the first order dispersion and the chromaticity (of sextupolar order). The total number of non-zero coefficients of the 9^{th} order transverse map is 4002, of which 2070 are horizontal and 1932 are vertical. These large numbers make the evaluation of the rms beam size very slow. A better approach for an optimization of the beam sizes is to consider the collimation section and the final focus separately.

Fig. 3 shows the rms beam sizes at the end of the collimation system versus the maximum order considered in the map, again for the nominal and the achromatic beams. It is obvious that the collimation section only needs a better adjustment of the chromaticity sextupoles. In this context this is efficiently achieved by matching the rms beam sigmas of order 2 to those of order 1 by varying the strengths of the chromaticity sextupoles. In principle, any optimization algorithm can be used to carry out this task. The code MAPCLASS [10] was written for this purpose with an implementation of the Simplex method [11]. The resulting beam sizes at the IP are shown in Fig. 4 versus order. A reduction of the second order sigmas is observed. More interestingly the contributions from orders above six have been significantly reduced both in the horizontal and

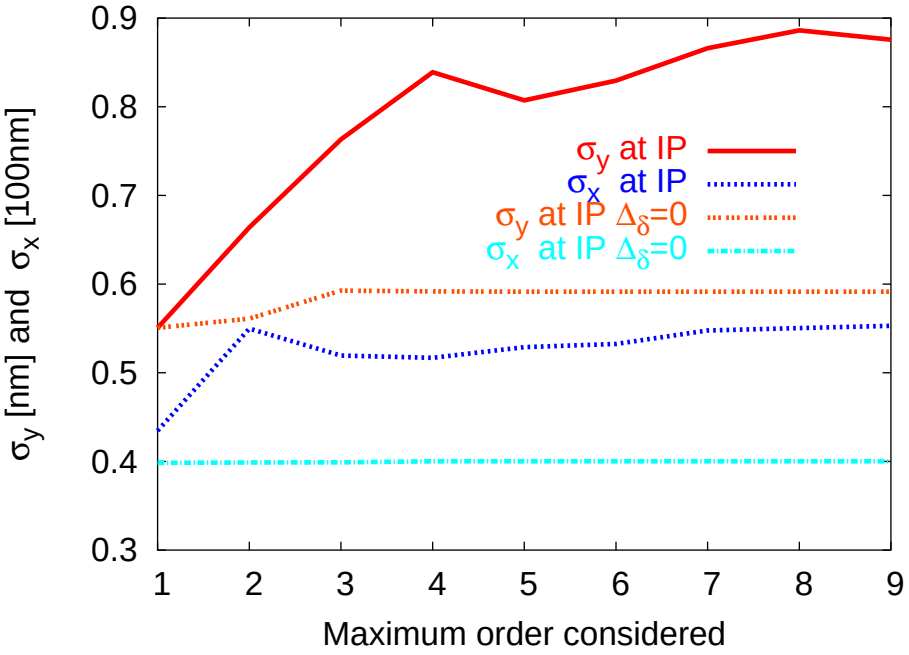

Figure 2: Horizontal and vertical rms beam sizes at CLIC Interaction Point as function of the maximum order considered in the transfer map. Both the nominal and achromatic beams are considered. The horizontal aberrations are purely chromatic and only a small part of the vertical aberrations are geometric.

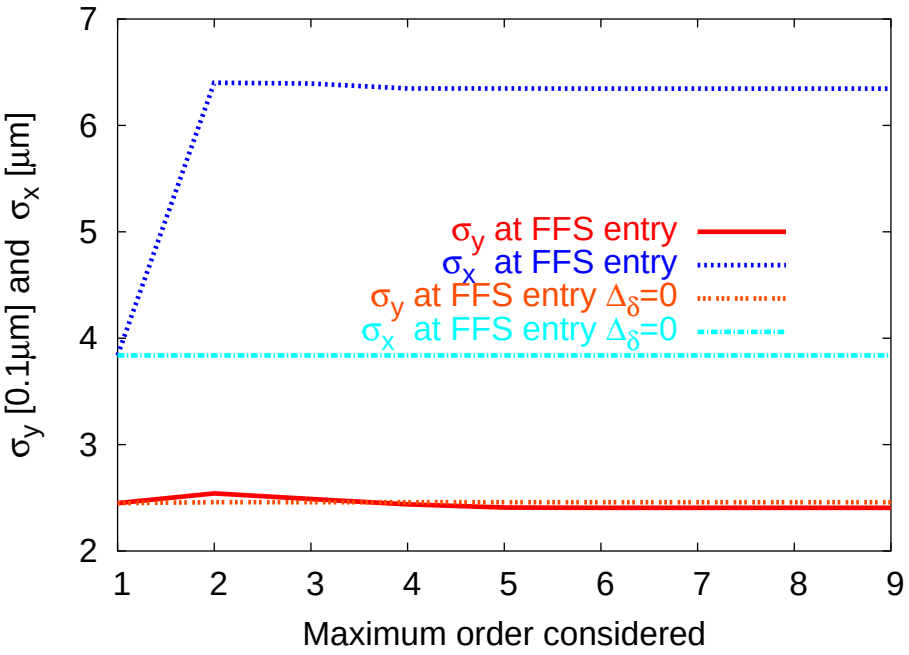

Figure 3: Horizontal and vertical rms beam sizes at the end of the CLIC collimation section as function of the maximum order considered in the transfer map. Both the nominal and achromatic beams are considered. The horizontal aberrations are purely chromatic.

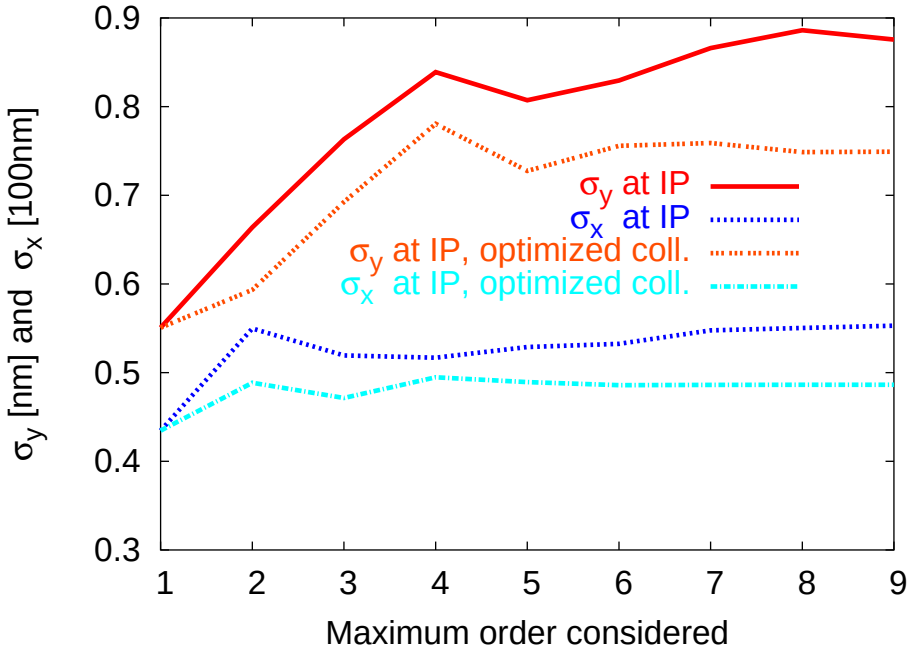

Figure 4: Horizontal and vertical rms beam sizes at the CLIC IP for the nominal collimation system and the one with optimized chromaticity.

vertical planes.

The remaining aberrations originate entirely in the FFS. The CLIC FFS has been designed based on the local chromaticity correction scheme proposed in [1]. This scheme basically consists of two pairs of sextupoles, one pair for the horizontal plane and the other for the vertical. The sextupoles of each pair are separated by 180° phase advance to compensate chromaticities and the subsequent geometrical aberrations. The compensation of the higher order aberrations can be achieved by correctors of the appropriate order arranged like the sextupoles. We assume that the pairs of sextupoles are combined magnets including octupolar and decapolar magnetic components. Using all these non-linear elements (sextupoles, octupoles and decapoles) in the FFS the rms beam sizes at the IP are minimized with the Simplex method. Initially the optimization works efficiently by truncating the map at 4^{th} order, however after a few iterations it is mandatory to increase the order up to $6\mathrm{th}$. The required computing time largely increases for this higher order. The result of the optimization of the FFS is shown in Fig. 5 together with the initial configuration. This confirms the compensation of the aberrations up to the higher orders.

Exactly the same algorithm can be used to optimize the linear parameters. Now that the non-linear aberrations have been compensated it is possible to focus more (decrease the beta functions at the IP) in order to reduce the beam size and gain luminosity. The rms beam sizes up to order 5 are minimized again using the Simplex method as before. The difference now is that only the strengths of the quadrupoles are used in the minimization. The result is shown in Fig. 6 together with the initial configuration. Both the horizontal and vertical beta functions have been reduced at the IP as can be seen at the first order of the plot. The horizontal beta-function at the IP has been reduced by 19%. The horizontal non-linear aberrations stay well compensated while in the vertical plane small aberrations have arisen as a consequence of the focusing. This implies that for further reduction of the beam sizes more iterations correcting non-linear and

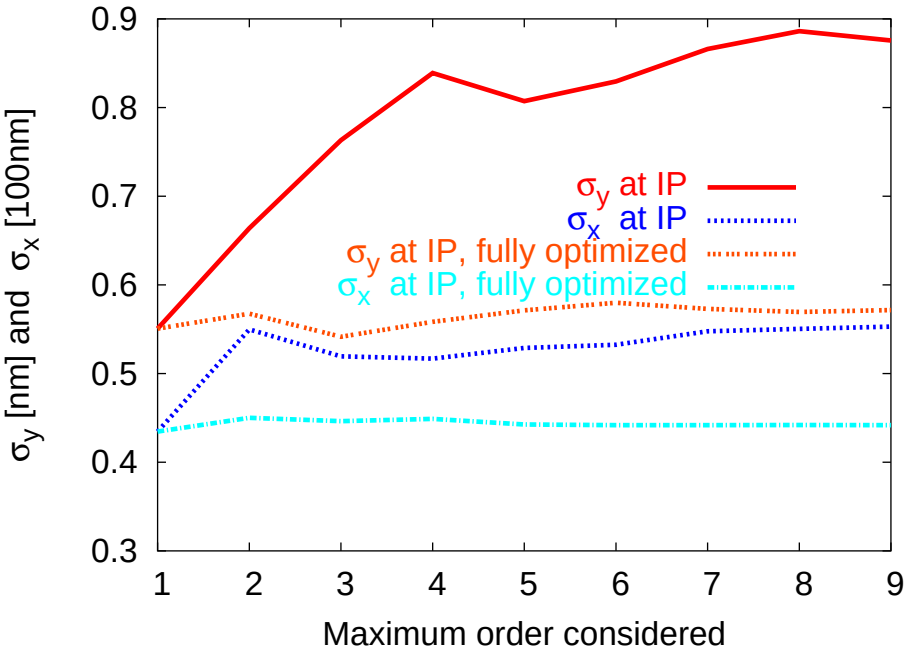

Figure 5: Horizontal and vertical rms beam sizes at the CLIC IP for the nominal BDS and the one fully optimized.

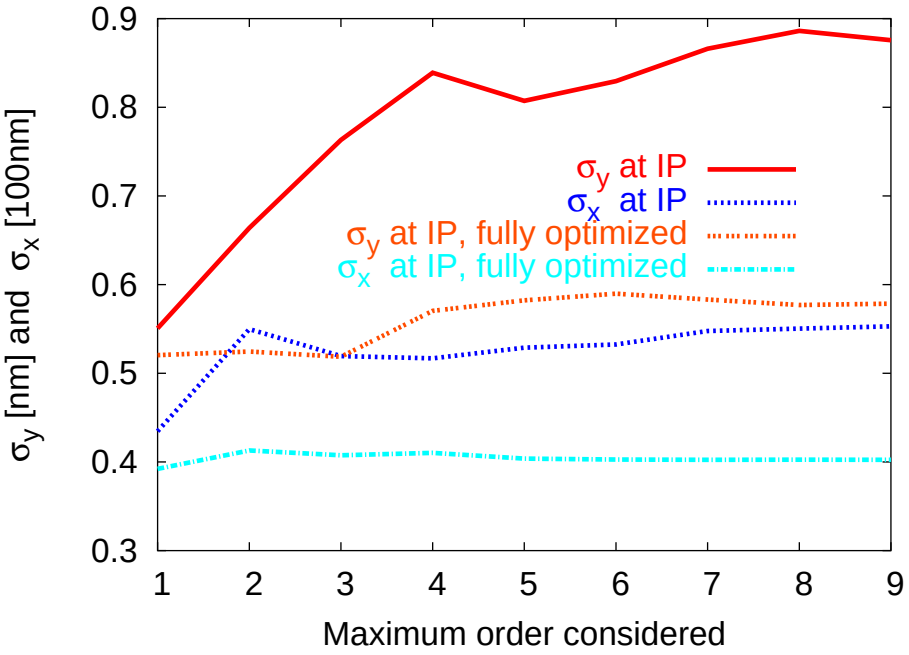

Figure 6: Horizontal and vertical rms beam sizes at the CLIC IP for the nominal BDS and the one linearly and non-linearly optimized.

$Case$	$\sigma_x^{rms}[nm]$ (no rad)	$\sigma_x^{rms}[nm]$ (rad)	$\sigma_y^{rms}[nm]$ (no rad)	$\sigma_y^{rms}[nm]$ (rad)	$L_{tot}[cm^{-2}/s]$	$L_{1\%}[cm^{-2}/s]$
Nominal	55	88	0.87	5.3	$6.15\ 10^{34}$	$2.65\ 10^{34}$

Table 1: CLIC nominal rms beam sizes and luminosities.

$Case$	$-\frac{\Delta\sigma_x}{\sigma_x^{rms}}$ (no rad)	$-\frac{\Delta\sigma_x}{\sigma_x^{rms}}$ (rad)	$-\frac{\Delta\sigma_y}{\sigma_y^{rms}}$ (no rad)	$-\frac{\Delta\sigma_y}{\sigma_y^{rms}}$ (rad)	$\frac{\Delta L_{tot}}{L_{tot}}$	$\frac{\Delta L_{1\%}}{L_{1\%}}$	$\frac{L_{1\%}}{L_{tot}}$
Nominal	0	0	0	0	0	0	43
Corrected collimation section	12	30	14	58	9	6	42
Corrected FFS non-linearities	20	35	35	69	31	19	39
Lower β_x and β_y at IP	27	37	34	64	45	29	38

Table 2: CLIC relative differences of beam sizes and luminosities for the different optimizations stages. All numbers are in percent units.

linear orders are required.

The real benefit of reducing the rms size at the IP is luminosity and therefore it has been computed for all the former stages of the optimization. Bunches of 10000 electrons have been tracked trough the CLIC BDS using PLACET [12]. The same beam parameters as mentioned above have been used and the effect of synchrotron radiation has been included, which is not taken into account by the described optimization procedure. The luminosity has been computed using the code GUINEA-PIG [13], see table 1 for the nominal values. The relative reduction of the beam sizes with and without radiation together with the relative luminosity increase is shown in table 2. The total luminosity (L_{tot}), the luminosity coming from the collisions with energy larger than 99% of the maximum energy ($L_{1\%}$) and their ratio ($L_{1\%}/L_{tot}$) are shown in the table. Both the total luminosity and the luminosity in the energy peak increase as the horizontal rms beam size gets smaller. It is interesting to see that after the first step the variation of the rms sizes with radiation is smaller than the variation of the rms sizes without radiation. Indeed the relative changes of the luminosities seem to be more related to the rms sizes without radiation, which are the ones used in the described optimization algorithm. The ratio of the luminosities slightly decreases but not in a significant manner.

4 Optimizing dispersion in the FFS

The presented optimization algorithm does not vary any variable having a direct impact on radiation, such as bending angles. In order to use these variables in the minimization procedure it would be mandatory to introduce analytical penalty functions that account for the effect of radiation in the final beam sizes. However, these penalty functions would be approximations that might not reflect the real impact of radiation in all possible configurations. Therefore another approach for the optimization of bending angles in the FFS has been used. The starting point is the above FFS configuration with the best performance. It is well known that the lower the dispersion is the less radiation is produced and the stronger the sextupoles need to be powered. There must be an optimum dispersion for which the combined effects radiation and sextupoles are minimum. The FFS is optimized using MAPCLASS for different levels of dispersion reduction and the luminosities are computed for the different cases as done above. Fig. 7 shows the resulting total and peak luminosities together with the required increase of sextupolar strength for the different levels of dispersion reduction. Table 3 contains the numerical values of the relative variation of the rms beam sizes and luminosities. The plot shows a peak in the lumi-

$Dispersion\ reduction\%$	$-\frac{\Delta\sigma_x}{\sigma_x^{rms}}$ (no rad)	$-\frac{\Delta\sigma_x}{\sigma_x^{rms}}$ (rad)	$-\frac{\Delta\sigma_y}{\sigma_y^{rms}}$ (no rad)	$-\frac{\Delta\sigma_y}{\sigma_y^{rms}}$ (rad)	$\frac{\Delta L_{tot}}{L_{tot}}$	$\frac{\Delta L_{1\%}}{L_{1\%}}$	$\frac{L_{1\%}}{L_{tot}}$
4.3	27	39	34	65	54	37	38
17.4	30	40	29	69	72	43	36
21.8	30	40	27	67	72	42	35
34.9	32	26	18	68	62	35	36

Table 3: CLIC relative differences of beam sizes and luminosities for the different dispersion reduction levels. All numbers are in percent units.

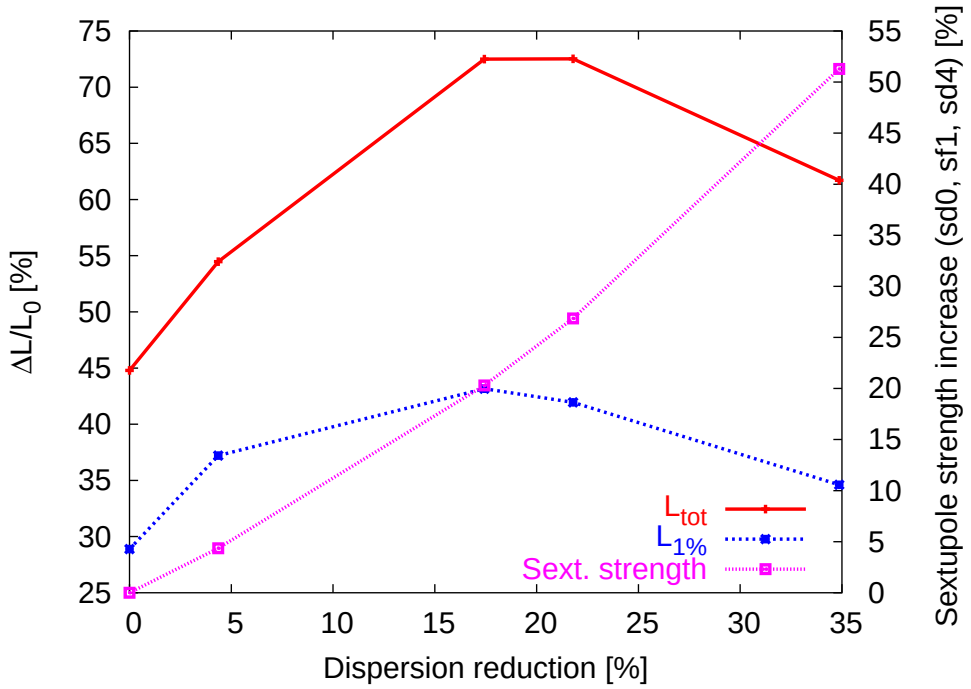

Figure 7: Relative luminosity versus dispersion reduction through the FFS.

nosities at about a 20% of dispersion reduction. The sextupole strength is not linear with the dispersion reduction, as could be predicted in a first approximation. The ratio of peak luminosity and total luminosity is reduced to 0.36 at the luminosity peak. The maximum gain of 72% in total luminosity confirms the usefulness of the presented algorithm for the optimization of beam lines.

Acknowledgments

Thanks to D. Schulte for setting up the PLACET and Guinea-Pig codes. F. Schmidt provided invaluable help concerning the use of MAD-X and PTC. Many thanks to H. Braun and F. Zimmermann for proofreading the manuscript and making useful suggestions. Thanks also to A. Faus-Golfe, J. Resta, D. Schulte, J. Payet, F. Ruggiero and F. Zimmermann for their motivation and useful discussions.

References

[1] P. Raimondi and A. Seryi, “Novel Final Focus Design for Future Linear Colliders”, Phys. Rev. Lett. **86**, 3779-3782 (2001).

[2] H. Grote and F. Schmidt, ”MAD-X - An Upgrade from MAD8”, CERN-AB-2003-024, ABP.

[3] E. Forest, F. Schmidt and E. McIntosh, “Introduction to the Polymorphic Tracking Code”, KEK Report 2002-3.

[4] F. Zimmermann et al., ”Final-Focus Schemes for CLIC at 3 TeV”, Proc. 18th International Conference on High Energy Accelerators (HEACC2001), Tsukuba, Japan, CERN-SL-2001-010 AP and CLIC Note 476 (2001).

[5] David C. Carey, “MINIMIZATION OF ABERRATIONS IN BEAM LINE DESIGN”, Proc. of the 1973 Particle Accelerator Conference, San Francisco, p. 493 (1973).

[6] F. Zimmermann, R. Helm, J. Irwin, ”Optimization of the NLC Final Focus System”, Proc. of the 1995 Particle Accelerator Conference, Dallas, 1995, p. 710 (1995)

[7] F. Zimmermann, “Magnet alignment tolerances in the SLC final focus system determined by Lie algebra techniques”, Nucleal Instruments and Methods A **364**, p. 231-238 (1995).

[8] O.Napoly, J.Payet, “DESIGNING THE TESLA INTERACTION REGION WITH L* = 5 M”, Proc. of the Nanobeam workshop, Lausanne, Switzerland 2002.

[9] A. Faus-Golfe, “Summary on Beam Delivery, Final Focus and Collimation Systems in Linear Colliders”, Proc. of the Nanobeam workshop, Lausanne, Switzerland 2002.

[10] R. Tomás, “MAPCLASS: A code to optimize high order aberrations”, CERN-AB-Note-017 ABP, 2006.

[11] J.A. Nelder and R. Mead, Computer Journal, 1965, vol **7**, pp 308-313.

[12] D. Schulte, et al., ”Simulation Package based on PLACET”, PAC2001, Chicago (2001); CERN/PS 2001 028 (AE), CLIC Note 482 (2001).

[13] D. Schulte, et al., ”Beam-Beam Simulations with GUINEA-PIG”, ICAP98, Monterey, CA., USA (1998).